TUNED LIQUID DAMPER (TLD) FOR SUPPRESSING HORIZONTAL MOTION OF STRUCTURES

-- Investigation on Nonlinear Waves in TLD and TLD-Structure Interaction --

Yozo FUJINO
Associate Professor

Benito M. PACHECO
Assistant Professor

Li-Min SUN
Graduate Student

Piyawat CHAISERI
Graduate Student

Department of Civil Engineering, University of Tokyo
7-3-1 Hongo, Bunkyo-ku, Tokyo 113, Japan
Tel. 3-812-2111 ext. 7722.
Fax. 3-813-5772

A new kind of damper named Tuned Liquid Damper (TLD) is explained that relies upon motion of shallow liquid in a rigid container for absorbing and dissipating the vibrational energy. Nonlinear equations of liquid motion inside rectangular TLD are developed based on shallow water wave theory, and a TLD-Structure Interaction model is proposed. Damping of liquid motion is evaluated semi-analytically. Liquid motion inside TLD under sinusoidal base excitation, and the effectiveness of a TLD mounted on a structural model subjected to an external force are experimentally investigated. Good agreement is found between the experiment and the theory. Among fundamental parameters of TLD, the influence of liquid viscosity is discussed in detail.

1. INTRODUCTION

Relatively light, flexible, and weakly damped structures are increasing in number because of growing use of high-strength materials and welded joints. Vibration of structures due to wind, earthquake and other disturbances then can create possible problems from the viewpoint of serviceability or even safety of bridges, towers, or buildings. The installation of various types of passive devices or so-called passive mechanical dampers is one way to suppress structural vibration.

This paper discusses a new type of passive mechanical damper, named Tuned Liquid Damper (TLD) (Fig. 1), which relies on motion of shallow liquid

inside a rigid container, for absorbing and dissipating structural vibration energy. Dampers using liquid motion have been in use in space satellites and marine vessels (Refs. 1-4). Recent growing interest in such a damper including TLD (for example, Refs. 5-10) is attributable to several potential advantages, including: low cost; easy installation especially in already existing structures which often have severe space constraints; adaptability to temporary use; easy trigger at small displacement amplitude; non-restriction to uni-directional excitation; and few maintenance requirements.

Studies so far on liquid dampers indicate their effectiveness. The performance of Tuned Liquid Damper (TLD) has been investigated by the authors using free-oscillation experiments (Ref. 7). It has been found that additional damping due to TLD is strongly dependent on amplitude of oscillation of liquid container. Nonlinear equations of liquid motion inside rectangular TLD were recently developed by the authors based on shallow water wave theory (Refs. 11-12), and are briefly explained in Section 2 below. It was found in Refs. 11-12 that the theory is in good agreement with the experiment in the region of relatively small vibration amplitude where no breaking of wave in TLD occurs and, hence, viscosity effect is dominant in energy absorption and dissipation.

Based on the theory of liquid motion referred to above, a TLD-Structure Interaction model is herein proposed to predict the performance of TLD. The performance of a rectangular TLD attached to a structure which is subjected to an external sinusoidal force is discussed. Experiment is carried out to confirm this model. The structural response with TLD is limited to a rather small amplitude range where no apparent wave breaking exists.

Application on a particular horizontally vibrating structure is also a goal of this study. Therefore, a commercially available, cheap and handy rectangular plastic container partially filled with water is tried as TLD, and the tested structure has horizontal natural frequency and damping similar to the object bridge girder. Prior to planned further experiments, the TLD-Structure Interaction model is used to numerically simulate structural response with attached TLD using high-viscosity liquid instead of water.

2. MODELLING OF LIQUID MOTION INSIDE RECTANGULAR TLD

The rigid rectangular tank (Fig. 2) has a length 2a, and the mean liquid depth is h. The origin of the Cartesian coordinate system (o-x-z) which is attached to the tank, is at the center of the mean liquid surface. A translational motion x_s (acceleration) is imposed on the tank in the x-direction. The following discussion is restricted to continuous surface condition (no wave breaking). The liquid particle motion is assumed to develop only in x-z plane. It is also assumed that the liquid is

incompressible, irrotational fluid, and the pressure p at liquid free surface is constant.

(1) Derivation of basic equations

The full equations governing the problem are the continuity equation

$$\frac{\partial u}{\partial x} + \frac{\partial w}{\partial z} = 0, \tag{1}$$

and the two-dimensional Navier-Stokes equations. u, w are the velocities of liquid particle (relative to the tank) in the x- and z-direction, respectively. For liquid having relatively small viscosity, the effect of internal friction in the fluid is appreciable only in the boundary layer near the solid boundary (Fig. 3). From this hypothesis, the liquid flow outside the boundary layer may be considered as potential flow, and the equations of motion become

$$\frac{\partial u}{\partial t} + u\frac{\partial u}{\partial x} + w\frac{\partial u}{\partial z} = -\frac{1}{\rho}\frac{\partial p}{\partial x} - \ddot{x}_s, \quad (-(h-h_b) \leq z \leq \eta) \tag{2}$$

$$\frac{\partial w}{\partial t} + u\frac{\partial w}{\partial x} + w\frac{\partial w}{\partial z} = -\frac{1}{\rho}\frac{\partial p}{\partial z} - g. \quad (-(h-h_b) \leq z \leq \eta) \tag{3}$$

where g is the gravity acceleration. Inside the boundary layer, the equations of motion are

$$\frac{\partial u}{\partial t} + u\frac{\partial u}{\partial x} + w\frac{\partial u}{\partial z} = -\frac{1}{\rho}\frac{\partial p}{\partial x} + \nu\frac{\partial^2 u}{\partial z^2} - \ddot{x}_s, \quad (-h \leq z \leq -(h-h_b)) \tag{4}$$

$$\frac{1}{\rho}\frac{\partial p}{\partial z} = -g, \quad (-h \leq z \leq -(h-h_b)) \tag{5}$$

where h_b is the thickness of boundary layer and is in the order of several percent of the representative length a. ρ and ν are the density and kinematic viscosity of liquid, respectively.

The boundary conditions are

$$u = 0, \quad \text{on the wall } (x = \pm a) \tag{6}$$

$$w = 0, \quad \text{at the bottom } (z = -h) \tag{7}$$

$$w = \frac{D\eta}{Dt} = \frac{\partial \eta}{\partial t} + u\frac{\partial \eta}{\partial x}, \quad \text{at the free surface } (z = \eta) \tag{8}$$

$$p = p_o = \text{constant} \quad \text{at the free surface } (z = \eta) \tag{9}$$

The velocity potential function Φ exists for the main flow. Based on the shallow water wave theory, Φ is assumed as (Ref. 13)

$$\Phi = F(x,t)\cosh(k(h+z)). \tag{10}$$

With the aid of Eq.(10), the vertical velocity w and its differentials can be expressed in terms of the horizontal velocity u. Governing equations are integrated (Ref. 12) with respect to z from bottom to free surface and the basic equations are obtained as

$$\frac{\partial \eta}{\partial t} + h\sigma \frac{\partial(\phi u(\eta))}{\partial x} = 0, \tag{11}$$

$$\frac{\partial}{\partial t}u(\eta) + (1-T_H^2)\, u(\eta) \frac{\partial}{\partial x}u(\eta) + g \frac{\partial \eta}{\partial x} + gh\sigma\phi \frac{\partial^2 \eta}{\partial x^2} \frac{\partial \eta}{\partial x}$$

$$= - \nu \int_{-h}^{-(h-h_b)} \frac{\partial^2 u}{\partial z^2}\, dz - \ddot{x}_s, \tag{12}$$

where $\sigma=\tanh(kh)/(kh)$, $\phi=\tanh(k(h+\eta))/\tanh(kh)$, $T_H=\tanh(k(h+\eta))$, $u(\eta)$ is the horizontal velocity of surface liquid particle, and k is wave number. Eq.(11) is the integral of the continuity equation while Eq.(12) is obtained from the equations of motion after eliminating the pressure p. The independent variables in these basic equations are $u(\eta)$ and η. The first term of the right hand side of Eq.(12), which is the integral of the second term of the right hand side of the equation of motion inside the boundary layer (Eq.(4)), is referred to as the dissipation term.

(2) Damping of liquid motion

The effect of liquid damping is significant on liquid motion near resonance. In the present formulation, assuming that the shear stress outside the boundary layer is very small, the dissipation term in Eq. (12) can be expressed as

$$\nu \int_{-h}^{-(h-h_b)} \frac{\partial^2 u}{\partial z^2}\, dz = -\frac{1}{\rho} \tau_b, \tag{13}$$

where $\tau_b = \rho\nu(\frac{\partial u}{\partial z})_{z=-h}$, is the bottom shear stress. In the present problem, Reynolds number is in the order of 10000 and the boundary layer is considered as a somewhat turbulent one. According to Jonsson's studies (Ref. 14), τ_b can be approximately expressed as

$$\tau_b = \frac{\rho}{2} f_b |u(\eta)|\, u(\eta). \tag{14}$$

The coefficient f_b in Eq. (14) is a wave friction factor associated with Reynolds number Re, which is defined as

$$Re = \frac{U^2(\eta)}{\omega\nu}, \tag{15}$$

where $U(\eta)$ is the amplitude of $u(\eta)$, which is unknown, while ω is the angular frequency of excitation. f_b can be expressed as (Ref. 14)

$$f_b = 2/\sqrt{Re} = 2\sqrt{\omega\nu} \,/\, U(\eta). \tag{16}$$

$U(\eta)$ can be eliminated from the equations by linearizing Eq. (14). Writing τ_b in the form

$$\tau_b = \frac{\rho}{2} f_b C_e u(\eta), \tag{17}$$

then the parameter C_e is determined by equating the energy loss per cycle by Eq. 14 to that by Eq. 17. From this consideration of energy loss per cycle,

$$C_e = \frac{8}{3\pi} U(\eta). \tag{18}$$

Thus, the dissipation term can be expressed in the form

$$\frac{\nu}{(\eta+h)} \int_{-h}^{-(h-h_b)} \frac{\partial^2 u}{\partial z^2} dz = - \frac{1}{(\eta+h)} \frac{8}{3\pi} \sqrt{\omega\nu}\, u(\eta). \tag{19}$$

So far, only the damping effect of bottom boundary layer has been considered in the derivation of basic equations. Vandorn (Ref. 15) reported that the damping of liquid motion in a container observed from experiment is larger than that computed on account of the bottom boundary layer. Miles (Refs. 16-17) has also studied the damping of surface wave in closed basin and suggested that the dissipation term can be multiplied by (1+(2h/b)+S), where b is the width of the tank, to account for dissipation due to side wall friction and liquid surface contamination. It is regarded that the friction of side wall boundary layer is the same as that of bottom boundary layer. 2h/b is an equivalent coefficient of the damping effect per width due to the side wall boundary layer. S is a "surface contamination" factor which can vary between 0 and 2. A value of unity for S will be used in this study, which corresponds to the establishment of "fully contaminated surface". Note that Ref. 18 also used S=1.

The dissipation term with the inclusion of the effects of side wall and free surface is

$$\frac{\nu}{(\eta+h)} \int_{-h}^{-(h-h_b)} \frac{\partial^2 u}{\partial z^2} dz = - \lambda\, u(\eta), \tag{20}$$

where $\lambda = \frac{1}{(\eta+h)} \frac{8}{3\pi} \sqrt{\omega\nu}\, (1+(2h/b)+S)$. (21)

According to the linear theory of the boundary layer (Ref. 19), λ is evaluated as

$$\lambda = \frac{1}{(\eta+h)} \frac{1}{\sqrt{2}} \sqrt{\omega\nu}\, (1+(2h/b)+S). \tag{22}$$

This value is somewhat smaller than that given by Eq.21 and is also used in the numerical simulation for comparison purposes.

(3) Numerical simulation method

The basic equations (Eqs.(11) and (12)) are discretized with respect to x into difference equations (staggered mesh) and can be solved numerically. The free surface waves originally possess a dispersion character, which is replaced by the dispersion relation produced by the discretization of the basic equations choosing a suitable division number n. The wave number k is taken as $\pi/2$, since the frequency around the first natural frequency is of main concern. In this paper, n is calculated using (Ref. 13):

$$n = \pi \,/\, \left(2\arccos\left(\sqrt{(\tanh(\pi\varepsilon)/(2\tanh(\pi\varepsilon/2))}\right)\right). \qquad (\varepsilon=h/a) \qquad (23)$$

After determining the division number n and with the corresponding boundary condition

$$u(\eta) = 0, \qquad (x = \pm a) \qquad (24)$$

the difference basic equations are solved using Runge-Kutta-Gill method and $u(\eta)$ and η can be computed.

(4) Base shear force of the tank due to liquid motion

Considering hydrostatic pressure and vertical acceleration effect only, the pressure p can be expressed as

$$\frac{1}{\rho}(p-p_0) = g(\eta-z) - \frac{1}{k^2}\left(\frac{\partial^2 u(\eta)}{\partial x \partial t} - \frac{\partial^2 u}{\partial x \partial t}\right). \qquad (25)$$

When η is known, integrating Eq. (25) with respect to z, the horizontal total pressure P can be calculated.

Neglecting the frictions of side wall and bottom, the base shear force of the tank due to liquid motion is

$$F = P_n - P_0. \qquad (26)$$

P_n and P_0 are the horizontal total pressures acting on the end walls of the tank due to liquid motion. These are functions of liquid free surface elevation near the end wall (Fig. 4).

3. SHAKING-TABLE EXPERIMENT AND COMPARISON WITH SIMULATION

(1) Experimental apparatus and procedure

In order to assess the validity of the model and to study the performance of liquid motion in TLD, a forced excitation experiment was carried out. A rectangular TLD tank was excited horizontally by a shaking table. A capacitance wave gage was used to measure liquid surface elevation near the end wall of the tank. For measuring base shear force of TLD tank, two load cells L1 and L2 were used to cancel the inertia force due to the TLD tank itself. Note that Mo in Fig. 5 is a mass equivalent to the mass of the tank. Output L1-L2 is the base shear force of TLD purely due to liquid motion. The evolution of liquid surface profile was photographed by a high speed camera.

A rectangular tank with length 2a=59.0cm (excitation direction) and width b=33.5cm, being made of 0.5cm thick acrylic plates was used (Fig. 6). The TLD tank was partially filled with plain water of h=3.0cm depth, corresponding to liquid depth ratio $\varepsilon=h/a=0.1$. From the linear wave theory, the natural fundamental frequency of liquid sloshing motion, f_w, was

$$f_w = \frac{1}{2\pi}\left(\frac{\pi g}{2a}\tanh\left(\frac{\pi h}{2a}\right)\right)^{1/2} = 0.458 \text{ Hz}, \qquad (27)$$

i.e., the natural period was T_w=2.18 sec. Water mass M_w was about 5.93 kg.

In the experiment, the TLD was quiescent at the start of table shaking. It was excited sinusoidally with various amplitudes. For four amplitudes of displacement of shaking table, A=0.1cm, 0.25cm, 0.5cm, and 1.0cm, the excitation frequency f was varied in the range of $0.8 < f/f_w < 1.5$.

The quantities measured in the experiment were: 1) displacement of shaking table, x_s; 2) liquid free surface elevation near the end wall, η_0; and 3) base shear force of TLD due to liquid motion, F. Data were converted from analog to digital, and were processed by a micro computer.

(2) Results of Experiment

Figure 7 shows sample time histories of displacement of shaking table, x_s; liquid free surface elevation near an end wall, η_0; and base shear force, F, with liquid motion at steady state. Even under the sinusoidal excitation, the wave forms of these time histories vary as the excitation frequency varies. Unsymmetrical wave form can be observed even under the excitation of small amplitude (Fig. 7(b)). At a certain excitation frequency, two or three waves can be observed in one cycle (for example, Fig. 7(c)).

Several nondimensional parameters are defined as follows for the presentation of results.

Liquid free surface elevation, η equals 0 at still liquid free surface. During liquid motion, η has at least one maximum value η_{max} (wave crest)

and one minimum value η_{min} (wave trough) in one cycle (Fig. 7). The nondimensional parameters η'_{max} and η'_{min} are defined as

$$\eta'_{max} = \eta_{max}/h; \qquad \eta'_{min} = \eta_{min}/h, \tag{28}$$

where h is liquid depth.

Under the sinusoidal excitation, base shear force F(t) has the same amplitude F_m either in positive direction or negative direction (Fig. 7). F_m is divided by the maximum inertia force of liquid as a solid mass under the sinusoidal excitation, and nondimensionalized:

$$F'_m = F_m/(M_w \omega^2 A). \tag{29}$$

The shaking table inputs energy into the TLD system, and the TLD itself dissipates energy due to liquid motion. When TLD is at steady state, it means that in each cycle the energy input into the TLD system equals the energy dissipation inside TLD. The energy input into the TLD, E_{input} can be calculated from the base shear force F and the displacement of shaking table x_s, which are both functions of time. Thus the energy dissipation per cycle ΔE can be calculated as

$$\Delta E = E_{input} = \int_t^{t+T} F(t)\, dx_s(t), \tag{30}$$

where T is the period of excitation, i.e. $2\pi/\omega$.

ΔE is nondimensionalized as follows,

$$\Delta E' = \Delta E/(\tfrac{1}{2} M_w (\omega A)^2) \tag{31}$$

It should be noted that $\frac{1}{2} M_w (\omega A)^2$ is just a reference value to nondimensionalize and not the energy of liquid motion.

(3) Comparison of numerical simulation with experimental result

For numerical simulation, the motion of TLD was assumed to be quiescent at t=0. The time increment was 1/60 of the excitation period of shaking table. The computation was carried on until 80 periods where liquid motion was regarded to have reached steady state.

Figure 8 presents the transient time history responses of base shear force, F for the input base amplitude 0.25cm. Numerical simulations corresponding to this case are also shown in Fig. 8 for comparison with experimental records. The response forms vary as the excitation frequency changes. At f/f_w=1.001, two waves in one cycle can be observed. This is the second mode of liquid motion, which is excited at an excitation frequency about one half of the second natural frequency of liquid motion.

At f/f_w=0.951, even the third mode can be observed clearly. Comparing the numerical simulation with the experimental results, good agreement can be found, i.e., the theory used here is satisfactory in accounting for the nonlinearity which induces higher modes of liquid motion.

Figure 9 shows some examples of force-displacement diagrams for the base displacement amplitude of 0.25cm. One can find in Fig. 9 that the simulation results agree well with those of the experiment.

In Fig.10, the nondimensionalized quantities, η'_{max}, η'_{min} (surface elevation), F'_m (maximum base shear force) and $\Delta E'$ (energy loss in TLD per cycle) are plotted for the frequency-ratio range of $0.9<f/f_w<1.3$. The solid lines in Fig. 10 show the simulation results using the damping parameter λ by Eq. 21, and the dotted lines using Eq. 22. The difference between Eq. 21 and Eq. 22 is found to be very small. Hereafter, λ given by Eq. 21 was used in the simulations.

All of the cases in the experiment indicate that the liquid motions possess strong nonlinearity (Fig. 10(a) to (d)). The resonant frequency ratio is greater than 1.00 even for the smallest input amplitude case (A=0.1cm). At a certain value of frequency ratio larger than 1.00, η'_{max} jumps down suddenly, indicating that the nonlinearity of liquid motion is "hardening spring" type. As the input amplitude increases, the resonant frequency ratio becomes larger, i.e., the nonlinearity becomes stronger. The resonant frequency ratio for the base amplitude of 0.1 cm is about 1.1 and increases to about 1.25 for the base amplitude of 1.0 cm.

The local peaks of η'_{max} (and also of F'_m and ΔE) for the frequency less than the resonant frequency can be found in Fig.12(a), (b) and (c) and these are due to appearance of higher modes as seen in Figs. 7-8.

For the relatively small amplitude excitation (0.1 cm, 0.25 cm, 0.5 cm), the simulation can well predict the experimental results, i.e., η'_{max}, η'_{min}, F'_m and $\Delta E'$.

For the input amplitude of 1.0 cm, breaking wave already exists (Fig. 10(d)). The simulation results do not agree with those of the experiment any more. The simulation overestimates η'_{max} and F'_m, although the resonant frequency ratio is well predicted. It should be noticed in Fig. 10(d) that the simulation underestimates $\Delta E'$ at range $1 < f/f_w < 1.25$. It may be explained that energy dissipation for the base displacement amplitude of 1.0cm is due to not only viscosity of liquid but also wave breaking. All these results indicate that the model used here is valid as far as the continuous free surface condition is satisfied.

For large excitation amplitude (Fig. 10(d)), F'_m and $\Delta E'$ are almost flat over a wide range of frequency.

4. TLD-STRUCTURE INTERACTION

(1) Interaction model

A single-degree-of-freedom (SDOF) structure with attached TLD (Fig.11) is proposed as TLD-Structure Interaction model. The equation of motion of the structure, which is subjected to sinusoidal external force $F_e = F_{eo} \sin \omega t$ and TLD base shear force F_{TLD}, can be expressed as

$$\ddot{x}_s + 2\omega_s \xi_s \dot{x}_s + \omega_s^2 x_s = \frac{1}{m_s}(F_{TLD} + F_e) \qquad (32)$$

where $\omega_s = (k_s/m_s)^{1/2}$, is the natural frequency; and $\xi_s = \frac{C_s}{2m_s \omega_s}$, is the damping ratio of the structure. F_{TLD} (or F in Eq. 26) is a function of the surface elevation η and the surface particle velocity $u(\eta)$ as described in Section 2, specifically in Eq. 25. The quantities η and $u(\eta)$ are functions of x_s (see Eqs. 11 and 12). Accordingly, at each time step in the numerical simulation, x_s, η and $u(\eta)$ are computed simultaneously from the three coupled equations (Eqs. 11, 12 and 32, coupled through Eq. 26).

(2) Forced excitation experiment

The structure in the interaction experiment was a platform vibrating in a shear-type horizontal motion (Fig.12). The total structural mass m_s was 168 kg. The natural frequency f_s was 0.91 Hz (natural period T_s = 1.10 sec). The structural damping ratio was 0.32%.

Aiming for a specific practical use, a commercially available plastic container, which approximately measured 25cm x 32cm x 11cm (height), was used as TLD.

The external sinusoidal force exerted to the structure was an inertia force of the oscillating part of an exciter, which was mounted on the platform. The external force amplitude was accordingly kept constant by keeping constant the amplitude of acceleration of the oscillating part relative to the platform. Excitation frequency (f) sweep was done with the frequency ratio f/f_s ranging from 0.85 to 1.15. The digitized data of structural displacement response x_s and liquid surface elevation at the end wall of the container η_0, at steady-state, were collected for the investigation.

The fixed amplitude of exciting force for that frequency range, was such as to cause the structure without TLD at resonance to vibrate at the amplitude A_0 of 1.0 cm at steady-state. After attaching TLD, structural response was affected as will be discussed below. Liquid depth used in the experiments was considered shallow, i.e., liquid depth ratio ε = liquid

depth/container half length = 0.2. No obvious wave breaking was visually observed.

(3) Discussion of TLD effectiveness in experiment and simulation

The experimental response of the structure with TLD (mass ratio μ = water mass m_w/structural mass m_s is about 1.0%), is shown in frequency response plots in Fig. 13 (• and ○). Note that in Fig. 13a and 13b the setting orientation of the container relative to the direction of platform motion is different, even though the mass ratio μ is almost the same. The results of the frequency sweep test toward higher frequency and backward show no effect of initial condition on wave and structural response. It can be seen both in Fig. 13a and 13b that at the region of resonance ($f/f_s \approx 1.0$), the vibration amplitude reduces drastically. Comparing Fig. 13a and 13b, however, it appears that the container with 2a=25cm and h=2.1cm has a better performance than that with 2a=32cm and h=3.6cm. This is caused by the difference in liquid damping λ of the two cases, as further discussed below.

Two clear peaks of the structural response can be seen. The first peak (at lower frequency ratio) fell below the corresponding structural response when without TLD; whereas the second peak rose a little. The results of the numerical simulation using TLD-Structure Interaction model, shown as lines in Fig. 13, agree quite well with the experiment. The few discrepancies that can be observed may be due to the irregularity in the shape of the container, which is not perfectly rectangular; e.g., the bottom is not flat. The numerical analysis is sensitive to the liquid depth h in terms of value and position of each peak in the frequency response. Further details are given in Ref. 20.

5. LIQUID VISCOSITY AS A TLD DESIGN PARAMETER

As in TMD (Tuned Mass Damper), the mass ratio, frequency ratio and liquid damping are controllable parameters in the design of TLDs. The first natural frequency, f_w of liquid motion in a rectangular container is a function of a and h:

$$f_w = \frac{1}{2\pi}\left(\frac{\pi g}{2a}\tanh\left(\frac{\pi h}{2a}\right)\right)^{1/2} \qquad (33)$$

For the tuning, i.e., $f_w/f_s=1.0$, the smaller container (smaller a) requires the shallower water depth h as Eq. 33 indicates.

The liquid damping is inversely proportional to the liquid depth, h as seen in Eq. 21, and consequently the smaller TLD has larger liquid damping when the same liquid is used. The results in Fig. 13 has indicated that for the more or less same mass ratio (μ=1%) the container with 2a=25cm (and

shallower h) was more efficient as a damper, than that with 2a=32cm. This can be attributed to the differences in liquid damping.

In Fig. 13a, there remains a response peak of the structure with TLD around 0.9Hz, suggesting that liquid damping is still less than the optimal value. Some smaller container (2a<25cm) may therefore be expected to show better performance as a damper. However, it should be noted that using smaller TLD container inherently leads to larger number of TLDs to attain the same mass ratio. This can create problems in container cost and space required for TLD installation.

Instead of changing the TLD tank size and corresponding liquid depth, the liquid damping λ may be also be changed by changing the liquid viscosity ν (see Eq. 21). Figure 14 shows the simulated effect of liquid viscosity on TLD-structure interaction (μ=1%, f_s=0.91Hz, 2a=25cm, h=2.1cm and ξ_s=0.32%). The structural response curves for various liquid viscosities of TLD (ν_w(plain water), $5\nu_w$, and $20\nu_w$) are plotted in Fig. 14. It appears in this example case that the structural response becomes almost flat over the frequency range considered, and is suppressed effectively when the liquid viscosity is $5\nu_w$. Indeed the liquid with appropriately high viscosity significantly improves the efficiency of TLD and this allows the use of relatively large size of TLD container. It should be noted, however that the optimal viscosity would depend upon the size of container.

Figure 15 shows the frequency response curves for comparing TLD and TMD effectiveness. Note that the TLD tank in this example is slightly different from that used in the preceeding example, and it was found in Ref. 12 that $\nu=20\nu_w$ is optimal in this case. Both dampers are optimized with a selected mass ratio of 1%. The optimal parameters of TMD are determined according to Ref. 21. It is found in Fig. 15 that, if optimized, the efficiency of TLD is comparable to TMD.

6. CONCLUDING REMARKS

The 2-dimensional basic equations of liquid motion were developed based on the "shallow water wave theory", in which the damping effects due to solid boundary friction and free surface contamination were included. No wave breaking is assumed to exist. The TLD-Structure Interaction model using a SDOF structure subjected to an external force F_e and TLD base shear force F_{TLD}, which can be calculated by using the developed basic equations, was proposed. Forced excitation experiments were conducted to investigate the performance of a TLD prototype using a commercially available rectangular plastic container in suppressing vibrations of a structure with 0.91 Hz natural frequency. The experimental results showed significant reduction of structure response around resonance (f/f_s= 1.00) region.

Good agreements between experimental and simulated results were observed, with only a few discrepancies that may be due to the irregularity in the shape of the container and to 3-dimensional effect of container width. The proposed model may be sufficient for designing real TLDs.

The theoretical simulations showed that one way to improve TLD performance would be to choose more suitable liquid viscosity. The effectiveness of TLD could be comparable to that of TMD. Development of high-viscous liquid suitable to TLD is a remaining subject of investigation, as well as the optimization of the various TLD parameters.

REFERENCES

[1] Bhuta, P. G. and Koval, L. R.: A Viscous Ring Damper for a Freely Precessing Satellite, Int. J. Mechanical Science, Vol. 8, pp. 383-395, 1966.

[2] Watanabe, S.: Method of Vibration Reduction, Proc. Japan Naval Arch. Soc. Symp., pp. 156-179, 1969. (In Japanese).

[3] Sayar, B. and Baumgarten J. R.: Linear and Nonlinear Analysis of Fluid Slosh Damper, AIAA J., Vol. 20, No. 11, pp,1534-1538, 1982.

[4] Matsuura, Y. et. al.: On a Mean to Reduce Excited-Vibration with the Sloshing in a Tank., Proc Japan Naval Arch. Soc., No. 160, pp. 424-432, 1986. (In Japanese).

[5] Modi, V. J. and Welt, F.: Vibration Control Using Nutation Dampers, Proc. Int. Conf. on Flow Induced Vibrations, England, pp. 369-376, 1987.

[6] Welt, F.: A Study of Nutation Dampers with Application to Wind Induced Oscillations, Ph. D. Thesis, The University of British Columbia, 204pp, 1988.

[7] Fujino, Y. et. al.: Parametric Studies on Tuned Liquid Damper (TLD) Using Circular Containers By Free-oscillation Experiment, J. Struc. Eng./Earthq. Eng., Proc. JSCE., No.398, 1988.

[8] Tamura, Y. and Fujii. K. et. al.: Wind-Induced Vibration of Tall Towers and Practical Applications of Tuned Sloshing Damper, Proc. Symposium/Workshop on Serviceability of Buildings, Ottawa, pp. 228-241, 1988.

[9] Sato, T.: Tuned Sloshing Damper. Japan J. Wind Eng., Vol. 32, pp. 67-68, 1987.

[10] Miyata, T. et. al.: Suppression of Tower-like Structures Vibration by Damping Effect of Sloshing Water Contained, J. Struc. Eng., JSCE, Vol.34A, pp.617-625, 1988. (In Japanese).

[11] Sun, L-M.: Simulation of nonlinear waves in rectangular Tuned Liquid Damper (TLD), Master Thesis, Dept. of Civil Eng., Univ. of Tokyo, Japan, 1988.

[12] Sun, L-M, Fujino, Y., Pacheco, B. M., and Isobe, M.: Nonlinear waves and Dynamic Pressures in Rectangular TLD, J. Struc. Eng./Earthq. Eng., Proc. JSCE. (submitted for possible publication).

[13] Shimizu, T., and Hayama, S.: Nonlinear Response of Sloshing Based on the Shallow Water Wave Theory". JSME International Journal. Vol.30, No.263, pp806-813. (or JSME, Vol.53(486), pp357-363, 1987. (In Japanese)).
[14] Jonsson, I. G.: Wave Boundary Layer and Friction Factors. Proc. 10th CCE, ASCE, pp.127-148, 1966.
[15] Vandorn, W. G.: Boundary Dissipation of Oscillatory Waves, J. of Fluid Mechanics, Vol. 24, part 4, pp.769-779, 1966.
[16] Miles, J. W.: Surface Wave Damping in Closed Basins, Proc. Royal Society of London, A 297, pp. 459-475, 1967.
[17] Miles, J. W.: Resonantly Forced, Nonlinear Gravity Waves in a Shallow Rectangular Tank, Wave Motion, Elsevier Science Publishers, B. V. (North Holland), 7, pp.291-297, 1985.
[18] Lepelletier, T. G. Raichlen, F.: Nonlinear Oscillations in Rectangular Tanks, J. of Engineering Mechanics, 114(1), ASCE. pp.1-23, 1988.
[19] Lamb, H.: Hydrodynamics, Cambridge Univ. Press, pp.619-621, 1932.
[20] Chaiseri, P., Fujino, Y., Pacheco, B. M. and Sun, L-M.: Interaction of TLD and Structure, J. Struc. Eng./Earthq. Eng., Proc. JSCE., (submitted for possible publication).
[21] Warburton G. B. and Ayorinde E. O.: Optimum Absorber Parameters for Simple Systems, Int. Jour. of Earthq. Eng. and Struct. Dynamics, Vol. 8, pp. 197-217, 1980.

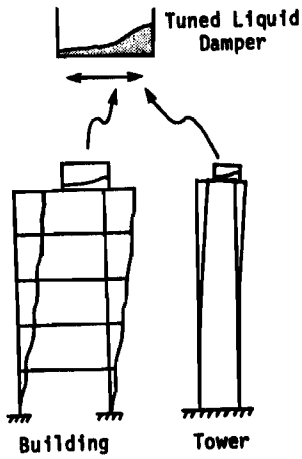

Fig. 1 Tuned Liquid Damper (TLD) installed on a building and tower

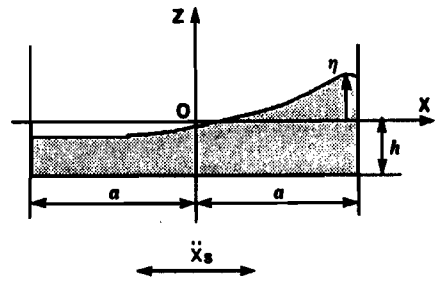

Fig. 2 Definition sketch for liquid motion in rectangular container

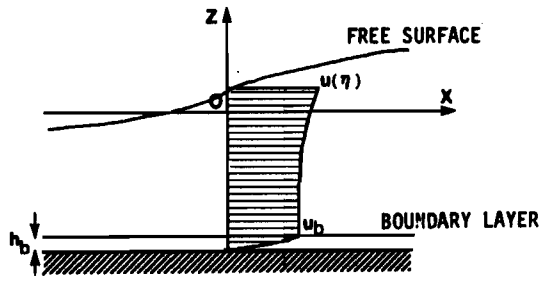

Fig. 3 The profile of liquid particle velocity in x-direction inside and outside the boundery layer

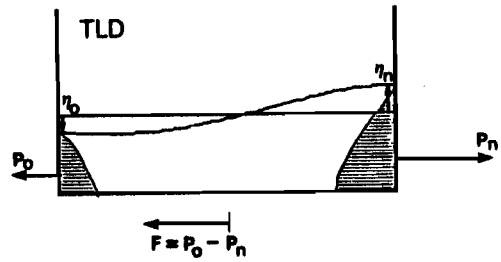

Fig. 4 Base shear force of container due to liquid motion

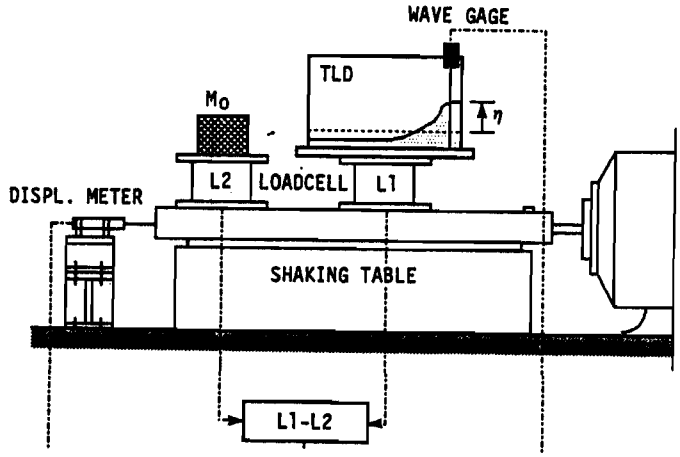

Fig. 5 The experimental apparatus

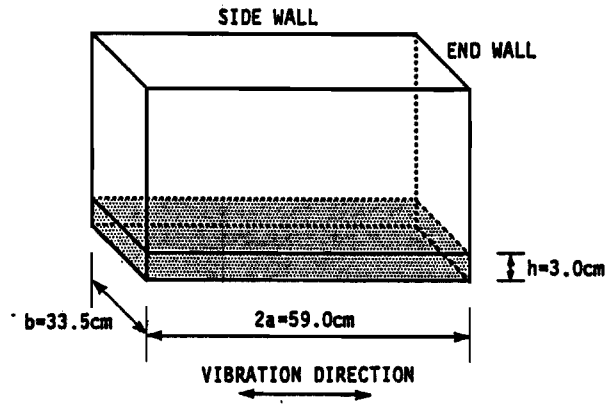

Fig. 6 TLD tank

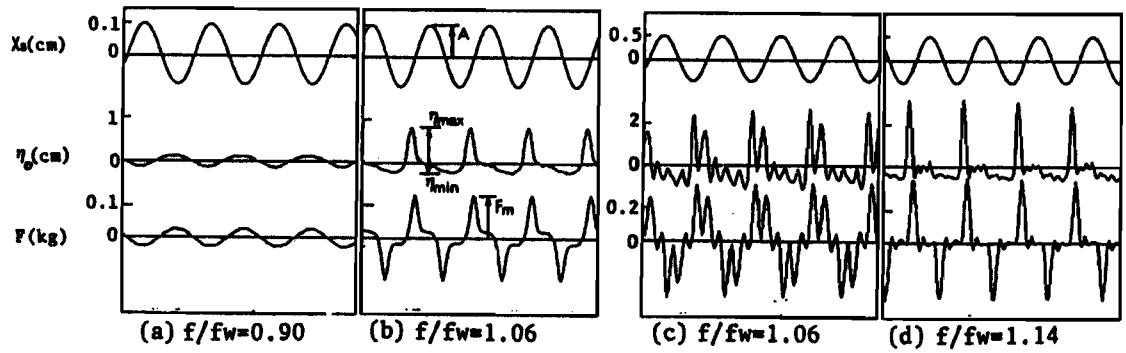

Fig. 7 Sample time histories of displacement of shaking table x_s, liquid surface elevation near the end wall η_0 and base shear force F

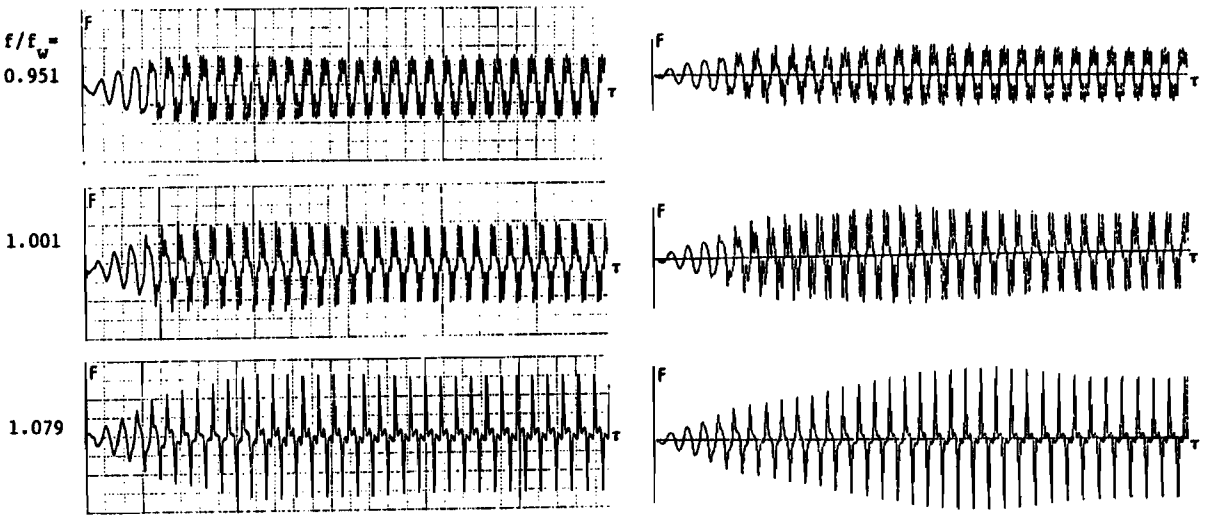

Fig. 8 The time histories of base shear force F
(base amplitude = 0.25 cm)

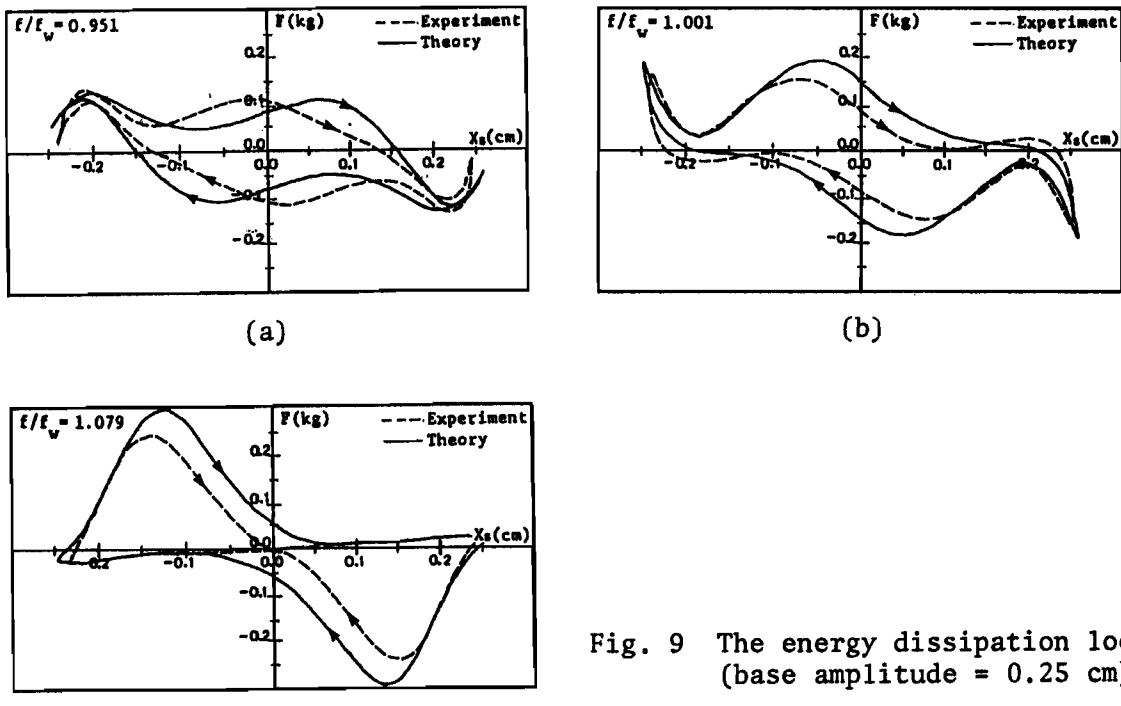

Fig. 9 The energy dissipation loops
(base amplitude = 0.25 cm)

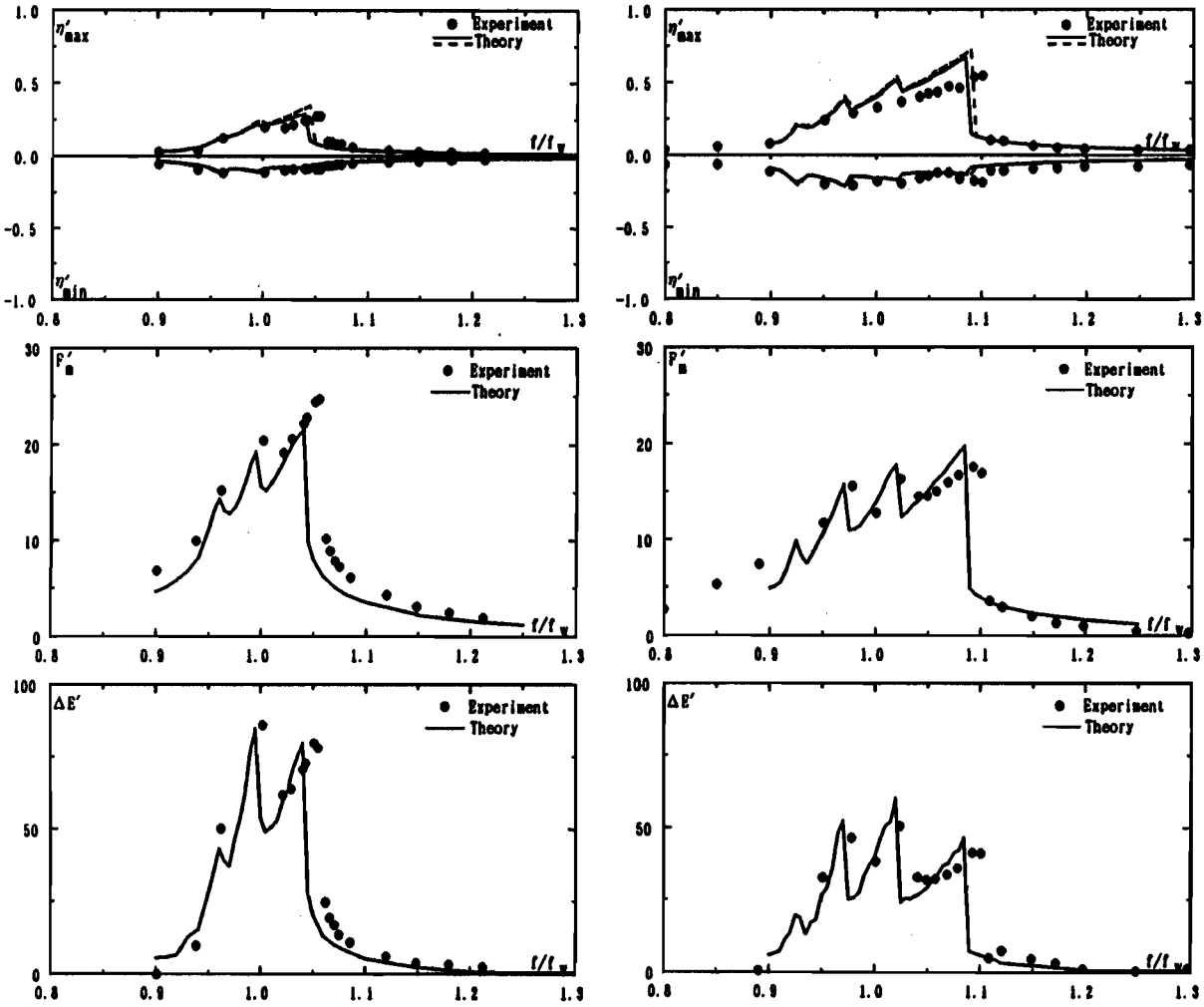

(a) base ampl.=0.1cm (b) base ampl.=0.25cm

Fig. 10 Frequency responses of η'_{max} and η'_{min}, F, and $\Delta E'$

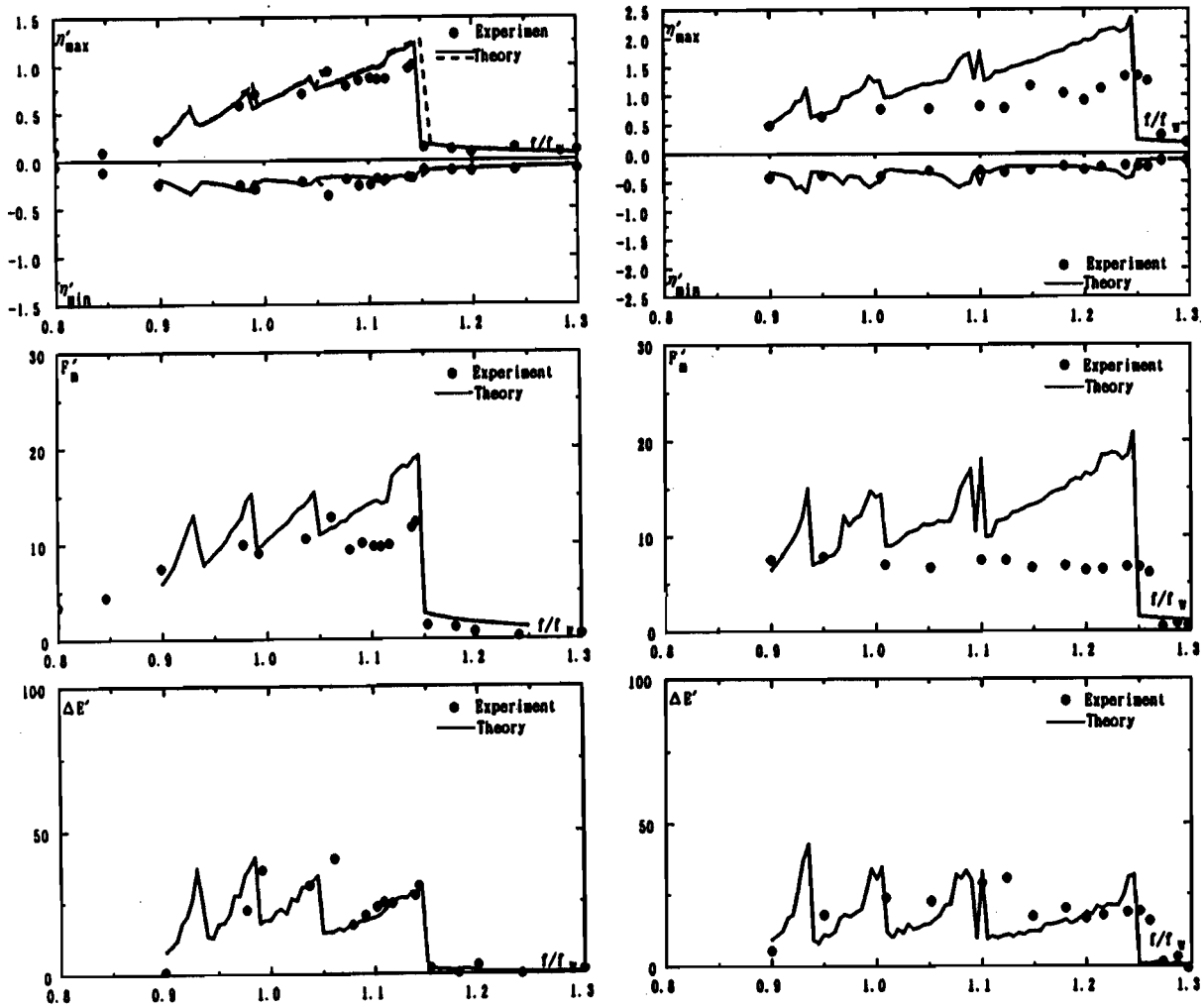

(c) base ampl.=0.5cm (d) base ampl.=1.0cm

Fig. 10 (Continued)

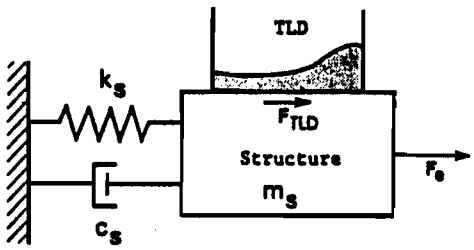

Fig. 11 TLD-Structures (SDOF) Interaction model

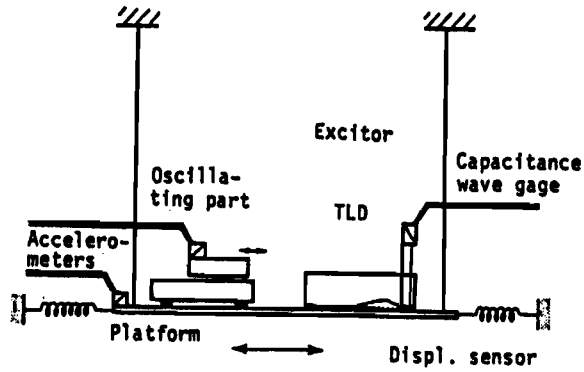

Fig. 12 Experimental set-up for TLD-structure interaction

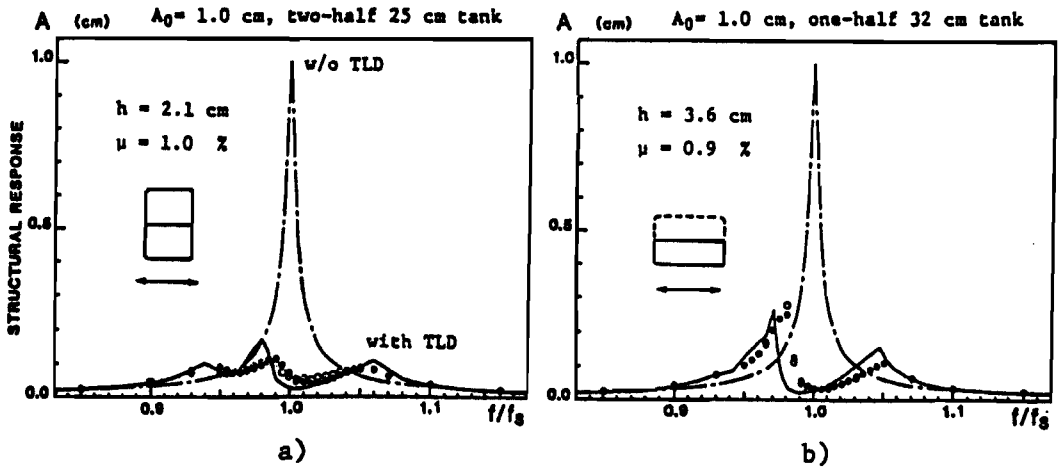

Fig. 13 Frequency response: numerical simulation and experiment (●sweep forward, ○sweep backward)

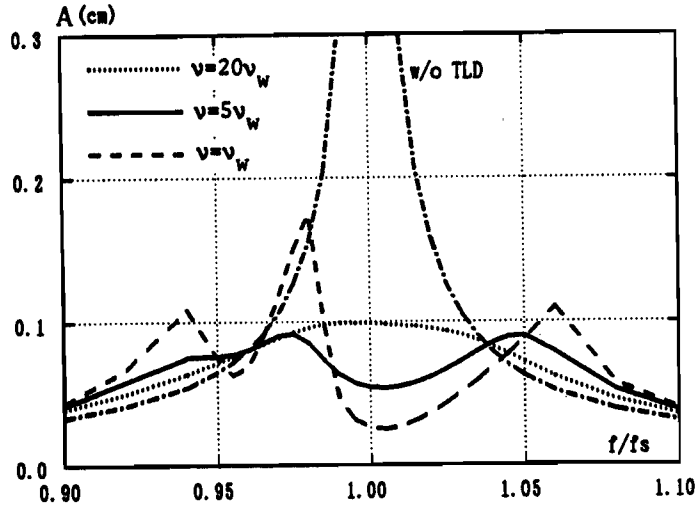

Fig. 14 Effect of liquid viscosity on TLD performance

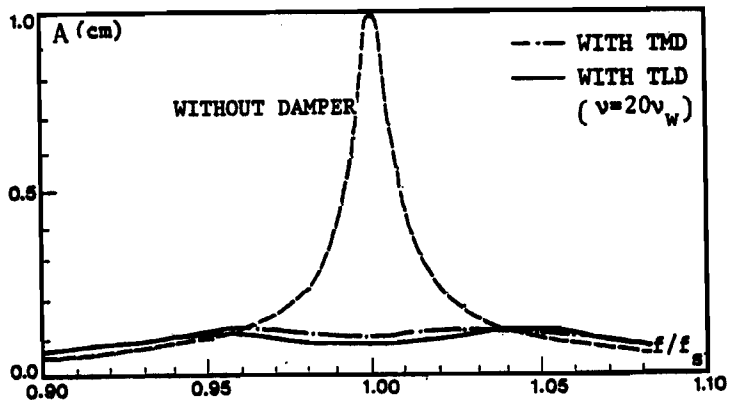

Fig. 15 Comparison of TLD and TMD